

Developing a Urinary Catheter with Anti-Biofilm Coated Surface Using Phyto-Assisted Synthesis of Zinc Oxide Nanoparticles

Reham M Goda^{1,*}, Ibrahim A Maghrabi², Mohamed F El-Badawy^{3,*}, Ahmed M Kabel⁴, Alaa A Omar⁵, Rasha M El-Morsi¹, Heba A Ramadan¹, Mohamed M Shohayeb¹

¹Department of Microbiology and Immunology, Faculty of Pharmacy, Delta University for Science and Technology, International Coastal Road, Gamasa, 11152, Egypt; ²Department of Clinical Pharmacy, College of Pharmacy, Taif University, Taif, 21944, Saudi Arabia; ³Department of Microbiology and Immunology, Faculty of Pharmacy, University of Sadat City, Sadat City, Menoufia, 32897, Egypt; ⁴Pharmacology Department, Faculty of Medicine, Tanta University, Tanta, 31527, Egypt; ⁵Nanomedicine Research Unit, Delta University for Science and Technology, International Coastal Road, Gamasa, 11152, Egypt

*These authors contributed equally to this work

Correspondence: Mohamed F El-Badawy, Department of Microbiology and Immunology, Faculty of Pharmacy, University of Sadat City, Sadat city, 32897, Menoufia, Egypt, Tel +20-103-205-9964, Email Mohamed.Elbadawy@fop.usc.edu.eg

Background: Biofilm-related infections represent one of the major challenging health problems that enhances antimicrobial resistance with subsequent treatment failure of catheter-associated urinary tract infections (CAUTIs).

Aim: This study aimed to employ and comprehensively characterize the use of nanoparticles to inhibit bacterial biofilm formation. Zinc oxide nanoparticles (ZnO-NPs) are considered one of the most important biofilm inhibitors.

Methods: The current study aimed to characterize the influence of the bioreductive green synthesis of ZnO-NPs using pomegranate peel extract on bacterial colonization to protect against urinary catheter infections. ZnO-NPs were investigated for their physico-chemical properties using UV, FTIR, Dynamic light scattering, and TEM. Catheters were coated with ZnO-NPs using *Pistacia lentiscus* (mastic), and the slow release of free zinc ions (Zn⁺²) from the ZnO-NPs-coated catheters, was evaluated using the ICP-AES technique.

Results: The current study revealed that catheter coated by ZnO-NPs exhibited a sustained antibiofilm activity against biofilm-forming and antibiotic-resistant clinical isolates of *Staphylococcus epidermidis*, *Staphylococcus aureus*, *Escherichia coli*, *Klebsiella pneumoniae*, *Proteus mirabilis*, and *Pseudomonas aeruginosa* strains.

Conclusion: The present study supports the efficiency of ZnO-NPs as a good candidate for prevention of biofilm formation.

Keywords: urinary catheters, biofilm, bacterial colonization, zinc oxide nanoparticles, catheter associated infection

Introduction

There is an urgent need for new effective methods to prevent and treat bacterial infections, particularly in light of the global problem of bacterial resistance. Regardless of the antibiotics' mechanism of action, bacteria can develop antimicrobial resistance by (a) changing the antibiotic's target by expressing genes coding for a different version of the target; (b) expressing enzymes that alter or degrade the drug; (c) preventing the uptake of antibiotics; (d) effluxing antibiotics; and (e) forming a biofilm around the bacterial cell.¹

Patients who use urinary catheters are more likely to have urinary tract infections (UTIs). Among the causes for the risk of getting catheter-associated infection (CAI), is the formation of bacterial biofilm on the catheter's surface. This bacterial biofilm is most likely to be formed seven days after catheterization and eventually causes UTI. The bacterial population causing the CAI is embedded in exo-polysaccharide matrix. The formed bacterial biofilm shields the bacteria against the surrounding environmental challenges like dryness, the human immune system and antimicrobial agents.²

As a result of emergence of bacterial resistance to antibacterial agents, nanoscale particles emerged as potential antibacterial agents. Nanoparticles have an increased surface area-to-volume ratio. Various nanoparticles formed of inorganic metals and their oxides (eg, zinc, zinc oxide, copper, copper oxide, titanium and titanium oxide) have been found to have antibacterial activity. Further, they are characterized by their stability, toughness, and long shelf life.³

Antibacterial nanoparticles can be created through chemical, physical, or biological means,⁴ and the vast majority of metal nanoparticles are created chemically. The chemical creation of metal nanoparticles is considered one of the source of environmental waste that creates significant health problems. This study aimed to imply green synthesis instead of chemical creation to generate metal nanoparticles. Green synthesis provides various advantages over chemical synthesis, as it is biocompatible, low in cost and safe for human health and the environment.⁵ Green synthesis relies on using plant extracts, bacteria, fungi, algae, etc, which provide catalytic activity and reduce the need for pricey and harmful chemicals.⁶

Metal nanoparticles attack both Gram-negative and Gram-positive bacterial pathogens via specific disruption of some essential processes necessary for cell growth.¹ Metal oxide ions are taken up by microbial cell membranes, where they interact with the functional groups of proteins and nucleic acid impairing their biological activities, leading to cellular structural changes and, ultimately, resulting in cell death.^{7,8} In addition, metal oxides also exert their antibacterial activity through the generation of reactive oxygen species (ROS) that subsequently cause changes in the bacterial cell wall, enzymes or DNA pathways.⁹

The stability, morphology, size distribution, surface functionality, and type of material(s) that is (are) employed in the synthesis metal and metal oxide nanoparticles are significantly effective and have major roles as antibacterials.¹⁰

ZnO-NPs have special characteristics, such as their strong adsorption ability, mechanical qualities, piezoelectric properties, magnetic properties, and high catalytic efficiency.¹¹ They have been proven, in numerous studies, to have strong antibacterial and anti-biofilm activity.^{12,13} Accordingly, this study employed a simple and straightforward approach for the preparation of green ZnO-NPs to inhibit bacterial biofilm formation on urinary catheters.

Materials and Methods

Media and Chemicals

Mueller–Hinton broth (MHB), Mueller–Hinton agar (MHA), Tryptic soy broth (TSB) and the following antibiotic discs; carbenicillin (CAR, 100µg), cefotaxime (CTX, 30µg), ceftriaxone (CRO, 30µg), ciprofloxacin (Cipro, 5µg), tobramycin (ToB, 10µg), erythromycin (E, 15µg), doxycycline (Do, 30µg), gentamycin (CN, 10µg), nitrofurantoin (F, 300µg), sulfamethoxazole-trimethoprim (SXT, 1.25/23.27µg), imipenem (IPM, 10µg) were purchased from Oxoid (Hampshire, UK). Zinc sulphate heptahydrate (ZnSO₄. 7H₂O) was used as a precursor to synthesize ZnO-NPs.

Preparation of Pomegranate (*Punica granatum* L.) Peel Extract

The identification of plant material was confirmed by Dr. Mohamed Saeed Refaey, an assistant professor of Pharmacognosy at the Faculty of Pharmacy, University of Sadat City, Egypt. Pomegranate peels were collected from the Egyptian market, washed for the first time with tap water to remove dust particles, then they were dried after rewashing for the second time with distilled water. The dried peels were ground to a fine powder. The powder (20 g) was soaked in 200 mL sterilized distilled water (dH₂O) and sonicated using a sonicator water bath for 30 min. The resulting pomegranate peel extract was filtered using Whatman filter paper No. 1 and used freshly for the synthesis of the target ZnO-NPs.

Green Synthesis of ZnO-NPs

ZnO-NPs were prepared using the phyto-assisted precipitation method proposed by Alneha et al¹⁴ with some modifications. Briefly, 10 mL of NaOH aqueous solution (3.75 M) were added to 25 mL of ZnSO₄.7H₂O aqueous solution (0.67 M) gradually over about 5 min, followed by dropwise addition of 30 mL of pomegranate peel extract. The mixture was stirred at room temperature for 90 min and then filtered. The precipitate was washed with ethanol, and then distilled water and left to dry at 37°C for 48 h. The dry powder was heated at 200°C for 3 h as shown in [Figure 1](#).

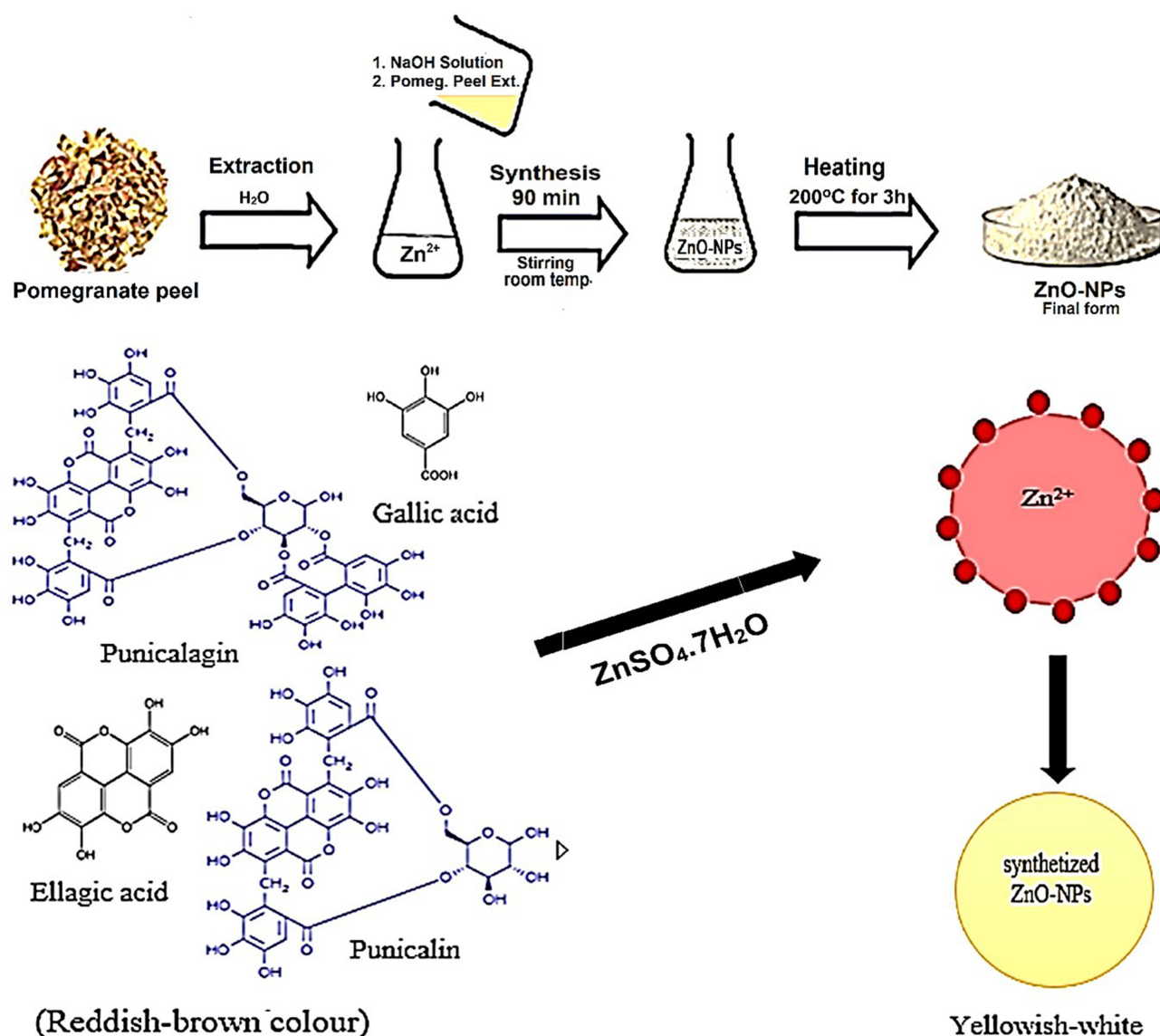


Figure 1 Schematic illustration of ZnO-NPs green synthesis using pomegranate peel extract.

Physico-Chemical Characterization of the Synthesized ZnO-NPs

Ultraviolet-Visible (UV-Vis) Spectroscopy

UV-Vis analysis was conducted using a UV-Vis spectrometer (UV-900I, Shimadzu, Japan). ZnO-NPs in dH₂O were sonicated for 10 min, and the spectra were determined over a wavelength range of 200–800 nm.

Dynamic Light Scattering (DLS)

The hydrodynamic diameter of the sonicated ZnO-NPs in dH₂O containing 10 mM KCl was characterized by DLS, at 25°C utilizing a Particle Sizing Systems (Inc. Santa Barbara, Calif., USA) at a scattering angle of 90°. Samples were suitably diluted to ensure free diffusion and unhindered Brownian motion of nanoparticles. All measurements were performed in triplicates.

Transmission Electron Microscope (TEM)

The copper grid was dipped into a sonicated solution of ZnO-NPs and allowed to dry at room temperature (RT). The shape and particle size distribution of ZnO-NPs were determined by TEM (Jeol, JEM2100, Japan).

Fourier Transform Infrared Spectrophotometry (FTIR)

FTIR (JASCO instrument, Japan) was used to identify the FTIR spectra of $\text{ZnSO}_4 \cdot 7 \text{H}_2\text{O}$ powder, pomegranate extract and ZnO-NPs over a wavelength range of 400 to 4500 cm^{-1} .

Bacterial Strains

The Gram-positive *Staphylococcus epidermidis* (*S. epidermidis*), *Staphylococcus aureus* (*S. aureus*) and the Gram-negative *Escherichia coli* (*E. coli*), *Klebsiella pneumoniae* (*K. pneumoniae*), *Proteus mirabilis* (*P. mirabilis*), and *Pseudomonas aeruginosa* (*P. aeruginosa*) strains were obtained from the culture collection of the Department of Microbiology and Immunology, Faculty of Pharmacy, Delta University for Science and Technology, Egypt.

Preparation of the Bacterial Inocula

Four separate colonies of each bacterial strain were transferred to a tube containing 5 mL of MHB. The broth was incubated at 37°C to a turbidity equivalent to 0.5 McFarland turbidity standards. Cultures were diluted 1:200 in broth to obtain an inoculum density of about 10^5 CFU/mL .

Antimicrobial Susceptibility Testing (AST)

The antibiogram for the tested strains was performed by a modified Kirby-Bauer disc diffusion method.¹⁵ Briefly, a sterile cotton swab was used to inoculate the surface of dried MHA plates. The inoculated plates were left to dry for 3–5 minutes. After that, antibiotic discs were placed onto the inoculated plates and lightly pressed with forceps. The plates were incubated in an inverted position for 18 h at 37°C . Plates were examined, and the diameters of the complete inhibition zones were measured and interpreted according to the guidelines of the Clinical Laboratory Standard Institute (CLSI).¹⁶

Antibacterial Activity of ZnO-NPs

A hole of 6 mm diameter was punched with a sterile cork borer into inoculated MHA plates. A volume of $50 \mu\text{L}$ of ZnO-NPs at a concentration of 50 mg mL^{-1} was added into each well. The plates were incubated at 37°C overnight. Each experiment was performed in triplicate and interpreted according to CLSI.¹⁶

Catheter Coating with ZnO-NPs

A sterile silicone urinary catheter was cut aseptically to a size of 1 cm long pieces that were washed for the first time with sterile dH_2O then ethanol and, thereafter, allowed to dry in a laminar flow cabinet. The sterile pieces of the catheter were dipped into a coating solution containing either *Pistacia lentiscus* (mastic) 50 mg mL^{-1} dissolved in chloroform or a mixture of ZnO-NPs (50 mg mL^{-1}) and mastic (50 mg mL^{-1}) dissolved in 1 mL chloroform. The treated catheter was gently stirred for 24 hours to achieve a coat on both the internal and external surfaces. Catheters were dried overnight at room temperature in glass petri dishes inside a laminar flow cabinet.¹⁷

The Inhibitory Effect of ZnO-NPs-Coated Catheters by Agar Diffusion Test

ZnO-NPs-coated catheters were dipped into MHA topped with 5 mL semisolid nutrient agar containing approximately 10^5 CFU mL^{-1} . The plates were left in the refrigerator for 1 h for prediffusion, and then incubated at 37°C for 18 h.¹⁸

Biofilm Formation Inhibitory Effect of ZnO-NPs-Coated Catheters

Each piece of the catheter was put into a test tube containing 5 mL sterile TSB containing about 10^5 CFU mL^{-1} of the tested bacterial strain. The tubes were incubated at 37°C for 24 h, and then they were removed and rinsed twice in phosphate-buffered saline (PBS) and placed into another tube containing 10 mL PBS. Tubes were vortexed and then sonicated in a sonication bath (MCS Digital ultrasonic cleaner) for 10 min to remove planktonic and non-adherent cells. The Bacterial cells released in the PBS were serially diluted into sterile PBS and plated onto the surface of dried MHA plates. The plates were incubated for 24 h at 37°C , and the viable count was calculated. Each test was done in triplicates. Positive control and the negative one were included in the experiment.¹⁸

Determination of Biofilm Inhibition by Scanning Electron Microscopy (SEM)

Biofilms were developed on pieces from ZnO-NPs-coated and uncoated control catheters as described above. The pieces of urinary catheter were washed with PBS and fixed with 2% glutaraldehyde for 2 h, followed by osmium tetroxide, tannic acid, and uranyl acetate. After dehydration with ethanol, the pieces of catheters were sputter-coated with Au-Pd (60:40 ratio)¹⁹ and examined for biofilm formation using SEM (XL3C SEM, Philips scanning microscope).

Zinc Ion (Zn^{2+}) Release from ZnO-NPs-Mastic-Coated Catheters

Pieces of ZnO-NPs coated catheters were impregnated in 5 mL of PBS (50 mm, pH 7.5) at 37°C. The catheter pieces were transferred every 24 h to a new tube containing a fresh PBS and incubated as mentioned above. This step was repeated for six days. To calculate the released amounts of Zn^{2+} , each tube was acidified with 0.5 mL concentrated nitric acid, and then treated with 60% perchloric acid to dissolve the precipitate. Each resulting clear solution was completed to 50 mL with deionized water and analysed for Zn^{2+} ions²⁰ using inductively coupled plasma atomic emission spectroscopy (ICP-AES) (PerkinElmer, USA).

Statistical Analysis

All experiments were carried out in triplicates, and all parameters were expressed as mean \pm standard deviation (\pm SD). Statistical Package for the Social Sciences (SPSS, software version 20, 2017, IBM Corporation, North Castle, NY, USA) was used for statistical analysis by applying one-way analysis of variance (ANOVA) followed by Kruskal Wallis with Dunnett's post hoc test. A P -value ≤ 0.05 was considered statistically significant, and all tests were conducted with a 95% confidence interval. The Shapiro–Wilk test was checked using the normality of the data distribution.

Results

UV-Vis Spectroscopy of the Synthesized ZnO-NPs

UV-Vis absorption spectra for the synthesized ZnO-NPs were conducted with a wavelength range of 200–800 nm, and its absorption peak maxima was observed at 290 nm (Figure 2). Moreover, UV-Vis spectroscopy was significantly contributed in ZnO-NPs characterization where it became clear that the distribution of nanoparticles was monodispersed.

DLS of the Synthesized ZnO-NPs

DLS analysis provides a size distribution based on the intensity and volume of particles. Data obtained revealed that the particle size distribution of ZnO-NPs was moderately multimodal with a polydispersity index of 0.58 ± 0.005 . The mean diameter was 70.9 ± 3.0 nm (Figure 3A). The zeta potential of ZnO-NPs was -12.85 kv (Figure 3B), which suggested an anionic surface charge.

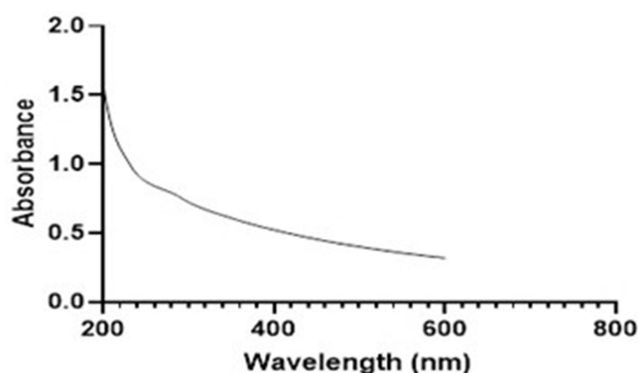


Figure 2 UV-Vis spectral analysis of synthesized ZnO-NPs.

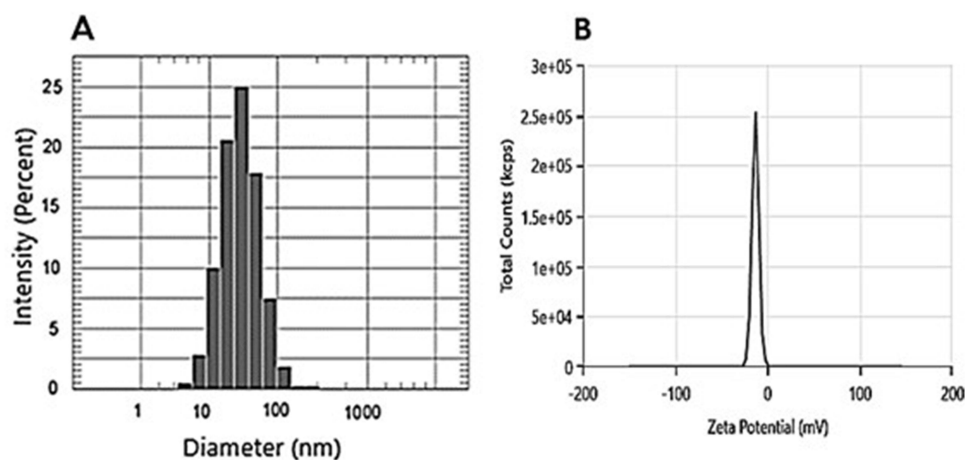


Figure 3 Particle size distribution (average mean diameter) measured by dynamic light scattering (DLS) for the synthesized ZnO-NPs (A). Zeta potential of the synthesized ZnO-NPs (B).

Transmission Electron Microscope (TEM)

The morphology and size distribution of the synthesized ZnO-NPs were determined by TEM to understand the crystalline size and characteristics of the nanoparticles. The obtained TEM micrographs of ZnO-NPs were approved to have different morphological structures like distorted nanospheres, nanopetals, and nanorod shapes as shown in Figure 4. The diameter of ZnO-N ranged between 28.13 and 114.3 nm. TEM micrographs showed the size of the nanoparticles in the average range or slightly smaller than that of the DLS technique (Figure 4).

FTIR of ZnO-NPs

Compared to the pomegranate peel extract, the intensity of all vibrational stretches in the synthesized ZnO-NPs decreased with a slight shift in wave numbers. The FT-IR analysis of synthesized ZnO-NPs revealed less pronounced peaks at 3471, 2725, 2305, and 1573 cm^{-1} and major bands at 1112 and 648 cm^{-1} (Figure 5). The band observed at 3471 cm^{-1} indicated the presence of N–H stretching of amines and that at 2725 cm^{-1} corresponded to C–H stretching of alkyls. Also, the bands at 2305 cm^{-1} and 1573 cm^{-1} indicated the presence of O–H stretching of carboxylic acid and N–H bends of amines, respectively. Not so prominent band appeared at the 1715–1727 cm^{-1} range, which confirms the presence of C=O carbonyl groups. Broad bands at 1609 cm^{-1} may be attributed to C=C of aromatic ring stretch. The absorption band observed at 1112 cm^{-1} corresponded to the presence of the C–N stretch of aliphatic amines and that at 648 cm^{-1} corresponded to the presence of the C–H bend of alkynes. Bands observed at 514 cm^{-1} indicated a stretch band of zinc and oxygen (Zn-O), confirming the synthesis of ZnO-NPs.

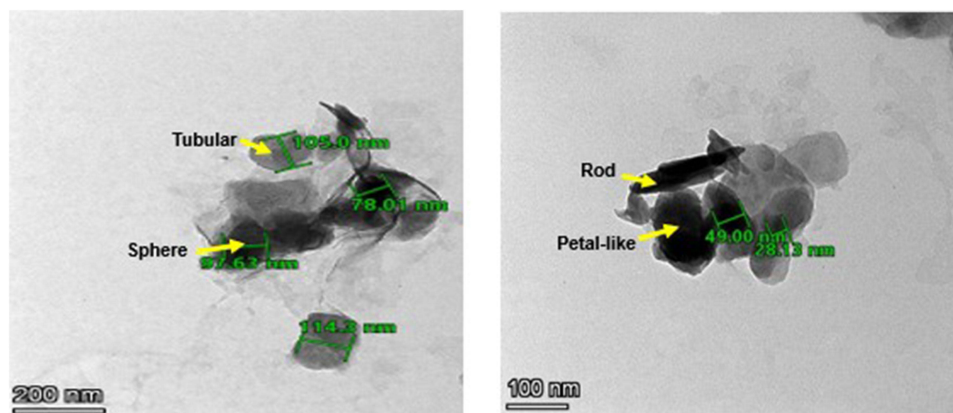


Figure 4 TEM micrographs of the synthesized ZnO-NP.

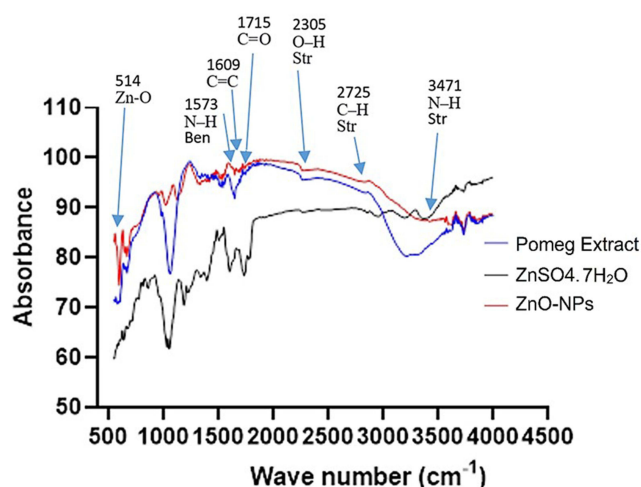


Figure 5 FTIR spectra of pomegranate extract (black), zinc sulphate $ZnSO_4 \cdot 7H_2O$ (blue) and ZnO-NPs (red).

AST

The AST for the tested pathogenic stains revealed that all the tested isolates were multidrug-resistant (MDR) and most of them were resistant to carbenicillin, cefotaxime, ceftriaxone, aztreonam, ciprofloxacin, tobramycin, erythromycin, doxycycline, nitrofurantoin, sulfamethoxazole/trimethoprim, and amikacin. On the other hand, all isolates were susceptible to gentamicin and imipenem, as shown in [Table 1](#).

The Inhibitory Effect of ZnO-NPs on the Investigated Clinical Isolates

ZnO-NPs were evaluated for their antimicrobial activity against six antibiotic-resistant and biofilm-forming clinical bacterial isolates by the cup-plate method. It was found that ZnO-NPs inhibited all the tested isolates, as shown in [\(Figure 6A and B\)](#).

Table 1 Color Coding for the Susceptibility Pattern of the Tested Clinical Isolates

Clinical Isolate	Antibiotic										
	β- Lactams				Aminoglycosides		Other Antibiotic Classes				
	CAR (100μg)	CRO (30μg)	CTX (30μg)	IPM (30μg)	TOB (10μg)	CN (10μg)	ERT (15μg)	F (300μg)	SXT (1.25/23.27μg)	DO (30μg)	CIP (5μg)
<i>E. coli</i>	R	R	S	S	R	S	R	R	R	S	R
<i>K. pneumoniae</i>	R	R	R	S	R	S	R	R	R	R	R
<i>P. mirabilis</i>	R	R	R	S	R	S	R	S	R	R	R
<i>P. aeruginosa</i>	R	R	R	S	R	S	R	S	R	R	R
<i>S. epidermidis</i>	R	R	S	S	R	S	R	R	R	R	R
<i>S. aureus</i>	R	R	S	S	R	S	R	R	R	S	R

Notes: . Red color indicates resistance pattern; Green color indicates susceptible pattern.

Abbreviations: AK, Amikacin; ATM, Aztreonam; CAR, Carbenicillin; CIP, CN, Gentamycin; Ciprofloxacin; CRO, Ceftriaxone; CTX, Cefotaxime; DO, Doxycycline; ERT, Erythromycin; F, Nitrofurantoin; IPM, Imipenem; R, Resistant; SXT, Sulfamethoxazole trimethoprim; S, Susceptible; TOB, Tobramycin.

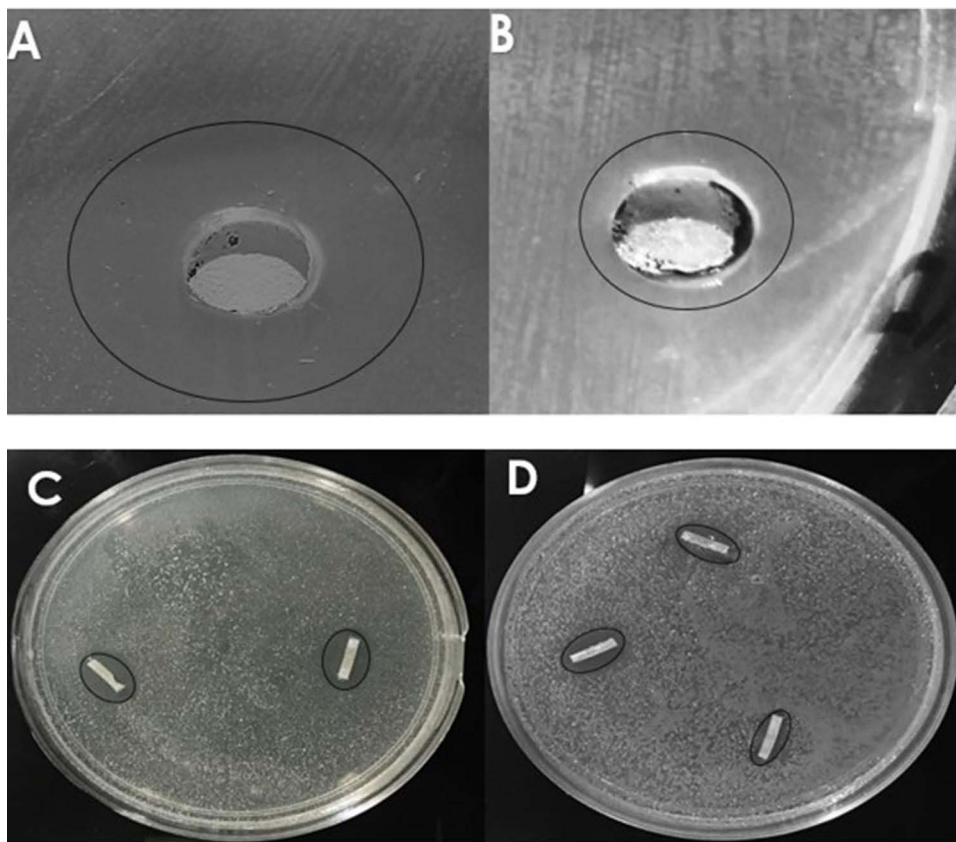


Figure 6 The inhibitory effect of ZnO-NPs on *Klebsiella pneumoniae* (A) and *Staphylococcus epidermidis* (B) by cup-plate method. The inhibitory effect of catheter pieces coated by ZnO-NPs on *K. pneumoniae* (C) and *S. epidermidis* (D).

The Inhibitory Effect of ZnO-NPs-Coated Catheter on the Investigated Clinical Isolates

The pieces of urinary catheter coated with ZnO-NPs were tested for their antimicrobial activity against the six biofilm-forming bacteria. It was found that catheters coated with ZnO-NPs exhibited inhibitory effect on the tested clinical isolates, as shown in (Figure 6C and D).

Biofilm Inhibitory Effect of ZnO-NPs-Coated Catheter

The inhibitory effect of ZnO-NPs on bacterial colonization of the coated urinary catheter pieces was evaluated by the viable count technique after the incubation of the catheters for 24 h, 48 h and 72 h. Viable counts of the tested bacteria colonizing the following (a) untreated catheter, (b) catheter coated with mastic only and (c) catheter varnished with both mastic and ZnO-NPs were summarized in Table 2.

The varnish of the mastic alone without ZnO-NPs exhibited a moderate inhibitory effect on the colonization of the catheter by the tested colonizing bacteria. The ZnO-NPs reduced the counts of the tested bacteria around two logs (Table 2).

SEM Analysis of the Catheter Pieces

The coating inhibitory effect on the colonizing activity of biofilm-forming bacteria on the urinary catheters coated with ZnO-NPs, using mastic as a varnish, was also evaluated by the examination of the catheters under SEM (Figure 7).

Bacterial colonization of the control catheters, and catheters varnished with mastic alone and with ZnO-NPs were examined by SEM. After 48 h, bacteria colonizing the control catheters appeared in clusters of *S. aureus* (Figure 7A) and stacked rods in the case of *K. pneumoniae* (Figure 7C). Lower numbers of colonizing bacterial cells were detected on

Table 2 The Inhibitory Effects of ZnO-NPs and Mastic on the Adherence of Different Types of Bacterial Cells to the Surface of 1 cm Silicon Catheter

Catheter Treatment	Time (Hour)	Bacteria					
		<i>S. epidermidis</i>	<i>S. aureus</i>	<i>E. coli</i>	<i>K. pneumoniae</i>	<i>P. aeruginosa</i>	<i>P. mirabilis</i>
		Log bacterial counts CFU mL ⁻¹ *					
Control	0	5.11 ± 0.611	5.13 ± 0.581	5.05 ± 1.059	5.14 ± 0.259	5.01 ± 0.450	5.22 ± 0.059
	24	6.86 ± 0.351	6.75 ± 0.208	6.86 ± 0.416	6.36 ± 0.115	6.32 ± 0.058	6.66 ± 0.231
	48	7.78 ± 2.180	7.68 ± 2.517	8.90 ± 0.319	8.60 ± 2.166	8.17 ± 1.500	8.30 ± 1.401
	72	8.86 ± 2.113	8.78 ± 1.660	9.36 ± 132.288	9.61 ± 2.167	9.18 ± 1.083	9.38 ± 2.376
Mastic	0	5.12 ± 0.412	5.23 ± 0.081	5.05 ± 1.009	5.11 ± 0.254	5.13 ± 0.440	5.02 ± 0.059
	24	5.90 ± 0.058	6.11 ± 0.058	6.85 ± 0.611	5.95 ± 0.058	5.30 ± 0.115	5.81 ± 0.076
	48	6.40 ± 0.200	6.15 ± 0.058	7.15 ± 12.583	6.18 ± 0.165	6.95 ± 0.208	6.90 ± 0.379
	72	6.90 ± 0.300	6.70 ± 0.289	7.54 ± 104.083	7.20 ± 1.638	7.91 ± 1.021	7.92 ± 1.511
ZnO-NPs/Mastic	0	5.02 ± 0.412	5.23 ± 0.254	5.05 ± 0.109	5.11 ± 0.081	5.03 ± 0.310	5.12 ± 0.059
	24	4.41 ± 0.351	4.30 ± 0.006	4.55 ± 0.014	4.66 ± 0.006	4.10 ± 0.003	4.60 ± 0.021
	48	5.19 ± 0.058	5.50 ± 0.144	5.91 ± 0.689	5.50 ± 2.822	5.80 ± 0.869	5.10 ± 1.418
	72	6.39 ± 0.511	6.20 ± 1.54	7.51 ± 135.769	7.11 ± 1.245	7.40 ± 1.133	7.18 ± 1.599

Note: *Results are expressed as mean ± SD (N = 3).

catheters coated with mastic alone. On the other hand, ZnO-NPs-mastic coats reduced the catheter colonization by *K. pneumoniae* and *S. aureus* (Figure 7B and D).

Zn²⁺ Sustained Release from ZnO-NPs-Coated Catheters

As shown in Figure 8, the in vitro release of Zn²⁺ was sustained for 6 days. The released amount of Zn²⁺ from the ZnO-NPs-mastic-coated catheters from the first to the sixth day ranged between 13.52 ± 0.13 and 17.72 ± 0.21 ppm with a slightly constant rate. These results revealed that the release rate depends on both the density and the linkage of ZnO-NPs with the mastic on the surface of the catheter.

Discussion

This study focused on the green fabrication of ZnO-NPs utilizing ZnSO₄ and pomegranate peel extract as a precursor. Pomegranate peel is rich in ellagitannins, flavonoids and other phytochemicals,²¹ that act as reducing agents to prevent NPs from agglomeration.²² Nanoparticles tend to aggregate, to reduce the number of active sites.²³ However, the observed zeta potential of ZnO-NPs of -12.85 kv, suggested an anionic surface due to the adsorption of phytochemicals, that reduced ZnO-NPs aggregation by keeping them dispersed.²⁴

UV, FTIR, DLS, and TEM were used for the physicochemical characterization, and all confirmed the formation of ZnO-NPs. The peak value obtained at 290 nm is within the 289 and 385 nm range, which is characteristic for ZnO-NPs.²⁵

TEM micrographs of the synthesized ZnO-NPs confirmed that they have tubular, spherical, rod, and petal-like morphology as previously reported.¹⁴ The average size of 70.9 nm and the hydrodynamic diameter of (140.5 nm) in the suspension were near or slightly larger than the average particle size observed in TEM (28.13–114.3 nm), due to its bias in measuring larger size particles or aggregates.²⁶

FTIR analysis was utilized in this study to determine the functional groups on the surface coating compounds of Zn-NPs. The O-H stretch bonds of free hydroxyl groups in pomegranate peel extract were verified by the FTIR spectrum, indicating the presence of ellagitannins and flavonoids. Ellagitannins and flavonoids of the peel extract are also rich in carbonyl groups with a high affinity for NPs.²¹ Compared to the pomegranate peel, the strength of all vibrational stretches in the prepared synthesized ZnO-NPs decreased with a minor shift in wavenumbers, signifying that the ZnO-NPs were effectively covered by the peel phytochemicals.

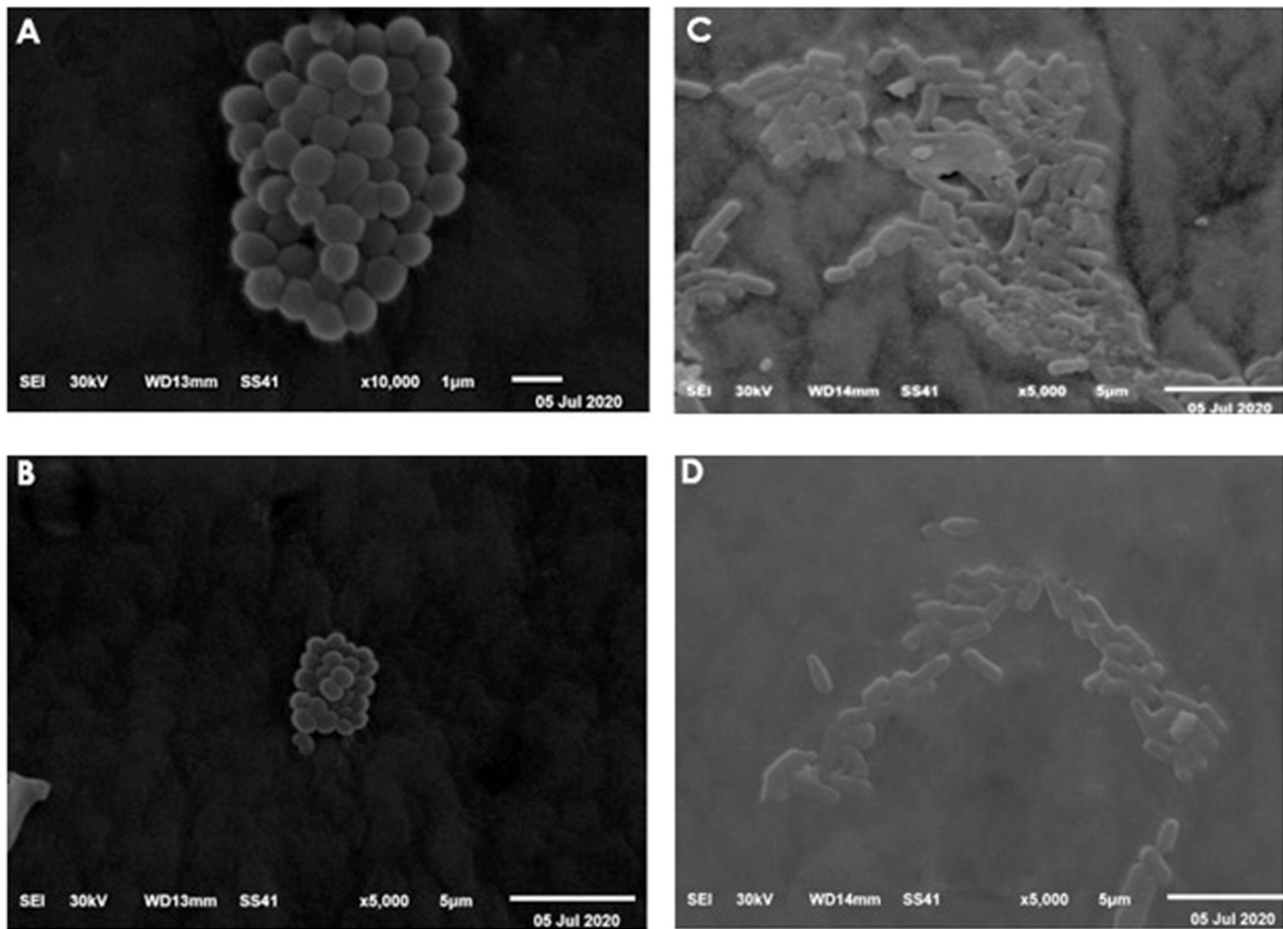


Figure 7 Scanning electron micrographs (SEM) for bacterial colonization of control catheters (**A** and **C**) and catheters varnished with mastic and ZnO-NPs (**B** and **D**), after 48h impregnation in tryptic soya broth inoculated with 10^5 CFU mL⁻¹ of *Staphylococcus aureus* (**A** and **B**) and *Klebsiella pneumoniae* (**C** and **D**).

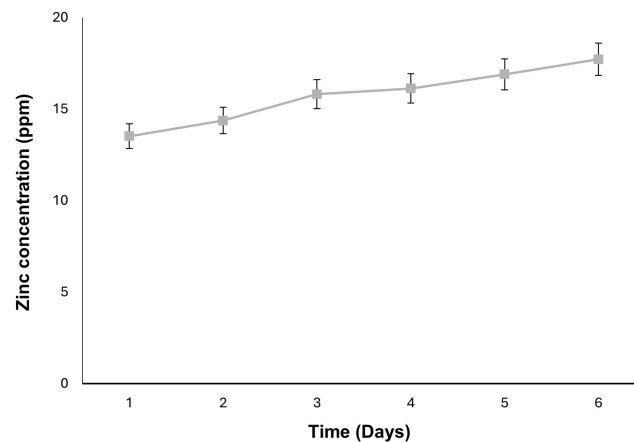


Figure 8 The release of Zn²⁺ from ZnO-NPs-coated catheters.

Bacterial biofilms have a significant impact on chronic and persistent infections. Biofilms hinder the immune system's response to bacteria cells and diminish the effectiveness of antibiotics.²⁷ Patients who need urinary catheters for extended periods are especially susceptible to biofilm-related catheter infections that may result in serious clinical consequences.²⁸

Developing novel agents that inhibit or disrupt biofilms may help in managing catheter-associated infections.²⁷ This study aimed to introduce a straightforward and facile technique for the synthesis of eco-friendly ZnO-NPs, to combat pathogenic bacteria and hinder their ability to colonize the surface of urinary catheters.

ZnO is one of the most important mineral elements for humans. It has a potent antimicrobial effect even at low concentrations.²⁹ Compared to other types of metal nanoparticles, ZnO-NPs offer special benefits because of their antibacterial and antioxidant qualities.³⁰

ZnO-NPs have a wide range of antibacterial activity, including clinical isolates of methicillin-resistant *S. aureus* (MRSA).^{11,12} In the same context, pomegranate peel extracts possess antibacterial, anti-inflammatory and antioxidant properties due to the presence of ellagitannins.³¹ In this study, pomegranate peel extract was used to synthesize ZnO-NPs.

The antimicrobial effect of ZnO-NPs was demonstrated against six selected Gram-negative and Gram-positive bacteria, involved in CAUTI. The broad-spectrum activity of ZnO-NPs against the tested bacteria differs from the report of Klink et al,³² who found that ZnO-NPs, synthesized using the microwave-heating crystallization technique, were ineffective against Gram-negative organisms like *E. coli*, *Salmonella enterica* and *Shigella sonnei* and their effect was limited only to Gram-positive organisms eg, *S. aureus*.

The broader range of activity, in this study, may be attributed to the potentiation of the antibacterial activity of ZnO-NPs by the presence of ellagitannins of pomegranate peel extract and the mastic; both of which have moderate antibacterial activities.^{33–35} The viable count technique demonstrated a moderate reduction in the counts of bacteria colonizing mastic-coated catheters, as previously reported.^{18,36} The mild antibacterial activity of mastic was also demonstrated by scanning electron microscopy, which revealed lower numbers of colonizing bacteria on the surface of mastic-coated catheters compared to catheters untreated with mastic. Mastic-coated catheters were capable of reducing the viable counts of colonizing bacteria by about one log.

ZnO-NPs-coated catheters inhibited biofilm formation and significantly reduced viable counts of bacteria ($p \leq 0.05$) by about two logs compared to control catheters. The inhibition of *S. aureus* biofilm formation by ZnO-NPs was previously reported by Abdelghafar et al.³⁷

The antimicrobial activity of ZnO-NPs has been attributed to the production of ROS, the loss of cellular integrity and the internalization of ZnO-NP with subsequent release of Zn^{2+} ions.³⁸ The generation of Zn^{2+} and hydrogen peroxide significantly contributes to the antibacterial action of ZnO-NPs.³⁸ The small size of ZnO-NPs enables them to enter the bacterial cell, whereby they interact with vital bacterial cell components such as DNA, proteins, and lipids.³⁹ The production of ROS, by ZnO, also compromises the membrane integrity and causes disorganization of bacterial intracellular structures.^{40,41}

In *S. aureus*, the antibiofilm activity of ZnO-NPs was attributed to a diminished formation of amyloid peptide fibrillation, which is an important component for the development of bacterial biofilm.³⁷

One important advantage of ZnO-NPs is their selective harmful effect on bacteria and their low harmful effects on human and animal cells.² This low cytotoxicity may be attributed to the slow release of metal ions at nontoxic levels from nanoparticles. In the current study, the release of Zn^{+2} from the ZnO-NPs-catheter pieces (1 cm long) was followed up for 6 days exhibiting that the release of Zn^{+2} was around 13.5–17.7 $\mu\text{g mL}^{-1}$ daily. The sustained release of Zn^{+2} from ZnO-NPs-coated catheters explains the observed significant reduction of viable counts of bacteria colonizing ZnO-NPs-coated catheters.

The tested Gram-positive and Gram-negative bacteria used in the study were resistant to 7–9 antibiotics of different classes. This suggests that antibiotic resistance mechanisms for those antibiotics are not protective against Zn^{+2} or ZnO-NPs. Generally, bacteria use other mechanisms of resistance to Zn^{+2} which include sequestration, active efflux, cell-wall modification and bioprecipitation.⁴² It seems that these mechanisms are uncommonly developed by pathogenic bacteria. Reports suggest that resistance to Zn and other heavy metals is more common in environmental microorganisms, though they may also be associated with resistance to some antibiotics.⁴³ It should be noted that *Pseudomonas* sp. commonly found in the environment is associated with catheter biofilm formation—a point to be considered when using ZnO-NPs-coated catheters.

Conclusions and Future Perspectives

The green synthesis of nanoparticles has become a dependable method due to its environmentally friendly nature. This technique was utilized to develop coated catheters. The fabricated antibiofilm ZnO-NPs coated catheter inhibited biofilm

formation in antibiotic resistant Gram-positive and Gram-negative clinical isolates. The activity of ZnO-NPs was potentiated by the use of mastic and pomegranate extract due to their mild antibacterial activities. The mastic coat was found to sustain the antibiofilm activity. Therefore, it may be concluded that ZnO-NPs-coated catheters could be a good candidate for preventing catheter-associated infections. However, further in vivo and toxicity studies should be carried out to demonstrate their in vivo competency.

Acknowledgment

We would like to thank Ms. Asmaa Ebadah and Ms. Amira ELRais, Department of Microbiology and Immunology, Faculty of Pharmacy, Delta University, Egypt, for their technical assistance.

Disclosure

The authors declare no conflicts of interest in this work.

References

1. Ifeanyichukwu UL, Fayemi OE, Ateba CN. Green synthesis of zinc oxide nanoparticles from pomegranate (*Punica granatum*) extracts and characterization of their antibacterial activity. *Molecules*. 2020;25(19):4521. doi:10.3390/molecules25194521
2. Shakerimoghaddam A, Ghaemi EA, Jamalli A. Zinc oxide nanoparticle reduced biofilm formation and antigen 43 expressions in uropathogenic *Escherichia coli*. *Iran J Basic Med Sci*. 2017;20(4):451. doi:10.22038/IJBMS.2017.8589
3. Ozdal M, Gurkok S. Recent advances in nanoparticles as antibacterial agent. *ADMET and DMPK*. 2022;10(2):115–129. doi:10.5599/admet.1172
4. Ukidave VV, Ingale LT. Green synthesis of zinc oxide nanoparticles from Coriandrum sativum and their use as fertilizer on Bengal gram, Turkish gram, and green gram plant growth. *Inter J Agron*. 2022;2022(1):8310038. doi:10.1155/2022/8310038
5. Faisal S, Jan H, Shah SA, et al. Green synthesis of zinc oxide (ZnO) nanoparticles using aqueous fruit extracts of *Myristica fragrans*: their characterizations and biological and environmental applications. *ACS Omega*. 2021;6(14):9709–9722. doi:10.1021/acsomega.1c00310
6. Yuvakkumar R, Suresh J, Nathanael AJ, Sundrarajan M, Hong S. Novel green synthetic strategy to prepare ZnO nanocrystals using rambutan (*Nephelium lappaceum* L.) peel extract and its antibacterial applications. *Mater Sci Eng*. 2014;41:17–27. doi:10.1016/j.msec.2014.04.025
7. Wang L, Hu C, Shao L. The antimicrobial activity of nanoparticles: present situation and prospects for the future. *Int J Nanomed*. 2017;12:1227–1249. doi:10.2147/IJN.S121956
8. Kumar MS, Saroja M, Venkatachalam M, Gudikandula K. *Acalypha indica* and *Curcuma longa* plant extracts mediated ZnS nanoparticles. *Mater Sci Res India*. 2019;16(2):174–182. doi:10.13005/msri/160210
9. Ruddaraju LK, Pammi SVN, Sankar Guntuku G, Padavala VS, Kolapalli VRM. A review on anti-bacterials to combat resistance: from ancient era of plants and metals to present and future perspectives of green nano technological combinations. *AJPS*. 2020;15(1):42–59. doi:10.1016/j.ajps.2019.03.002
10. Khezerlou A, Alizadeh-Sani M, Azizi-Lalabadi M, Ehsani A. Nanoparticles and their antimicrobial properties against pathogens including bacteria, fungi, parasites and viruses. *Microb Pathog*. 2018;123:505–526. doi:10.1016/j.micpath.2018.08.008
11. El-Fallal AA, Elfayoumy RA, El-Zahed MM. Antibacterial activity of biosynthesized zinc oxide nanoparticles using Kombucha extract. *SN Appl Sci*. 2023;5(12):332. doi:10.1007/s42452-023-05546-x
12. Akbar A, Sadiq MB, Ali I, et al. Synthesis and antimicrobial activity of zinc oxide nanoparticles against foodborne pathogens *Salmonella typhimurium* and *Staphylococcus aureus*. *ISBAB*. 2019;17:36–42.
13. Banerjee S, Vishakha K, Das S, et al. Antibacterial, anti-biofilm activity and mechanism of action of pancreatin doped zinc oxide nanoparticles against methicillin resistant *Staphylococcus aureus*. *Colloids Surf B Biointerfaces*. 2020;190:110921. doi:10.1016/j.colsurfb.2020.110921
14. Alnehia A, A-B A-O, Al-Sharabi A, Al-Hammadi A, Ws S. Pomegranate peel extract-mediated green synthesis of ZnO-NPs: extract concentration-dependent structure, optical, and antibacterial activity. *J Chem*. 2022;2022(1):9647793. doi:10.1155/2022/9647793
15. Hudzicki J. Kirby-Bauer disk diffusion susceptibility test protocol. *ASM*. 2009;15(1):1–23.
16. Aggarwal P, Saxena S, Nagi N. Possible impact of revisions in disc diffusion breakpoints for aminoglycosides and piperacillin/tazobactam in the 33rd edition of CLSI M100 document on clinical reporting and use in Indian settings with low susceptibility. *Indian J Med Microbiol*. 2024;49:100602. doi:10.1016/j.ijmm.2024.100602
17. Chaiban G, Hanna H, Dvorak T, Raad I. A rapid method of impregnating endotracheal tubes and urinary catheters with gendine: a novel antiseptic agent. *J Antimicrob Chemother*. 2005;55(1):51–56. doi:10.1093/jac/dkh499
18. Goda R, Shohayeb M. Use of *Pistacia lentiscus* mastic for sustained-release system of chlorocresol and benzoic acid for in vitro prevention of bacterial colonization of silicon urinary catheter. *Lett Appl Microbiol*. 2021;73(5):599–606. doi:10.1111/lam.13541
19. Hachem R, Reitzel R, Borne A, et al. Novel antiseptic urinary catheters for prevention of urinary tract infections: correlation of in vivo and in vitro test results. *Antimicrob Agents Chemother*. 2009;53(12):5145–5149. doi:10.1128/AAC.00718-09
20. Moon C-S, Zhang Z-W, Shimbo S, et al. A comparison of the food composition table-based estimates of dietary element intake with the values obtained by inductively coupled plasma atomic emission spectrometry: an experience in a Japanese population. *J Trace Elem Med Biol*. 1996;10(4):237–244. doi:10.1016/S0946-672X(96)80041-1
21. Tomás-Barberán F, Gil-Izquierdo A, Moreno D. Bioavailability and metabolism of phenolic compounds and glucosinolates. *Desig Funct Foods*. 2009;2009:194–229.
22. Ramesh M, Anbuvanann M, Viruthagiri G. Green synthesis of ZnO nanoparticles using *Solanum nigrum* leaf extract and their antibacterial activity. *Spectrochim Acta a Mol Biomol Spectrosc*. 2015;136:864–870. doi:10.1016/j.saa.2014.09.105

23. Modirshahla N, Hassani A, Behnajady MA, Rahbarfam R. Effect of operational parameters on decolorization of Acid Yellow 23 from wastewater by UV irradiation using ZnO and ZnO/SnO₂ photocatalysts. *Desalination*. 2011;271(1–3):187–192. doi:10.1016/j.desal.2010.12.027
24. Vimala K, Sundarraj S, Paulpandi M, Vengatesan S, Kannan S. Green synthesized doxorubicin loaded zinc oxide nanoparticles regulates the Bax and Bcl-2 expression in breast and colon carcinoma. *Proc Biochem*. 2014;49(1):160–172. doi:10.1016/j.procbio.2013.10.007
25. Amuthavalli P, Hwang J-S, Dahms H-U, et al. Zinc oxide nanoparticles using plant *Lawsonia inermis* and their mosquitocidal, antimicrobial, anticancer applications showing moderate side effects. *Sci Rep*. 2021;11(1):8837. doi:10.1038/s41598-021-88164-0
26. Modena MM, Rühle B, Burg TP, Wuttke S. Nanoparticle characterization: what to measure? *Adv Mater*. 2019;31(32):1901556. doi:10.1002/adma.201901556
27. Valadbeigi H, Sadeghifard N, Kaviar VH, Haddadi MH, Ghafourian S, Maleki A. Effect of ZnO nanoparticles on biofilm formation and gene expression of the toxin-antitoxin system in clinical isolates of *Pseudomonas aeruginosa*. *Ann Clin Microbiol Antimicrob*. 2023;22(1):89. doi:10.1186/s12941-023-00639-2
28. Pelling H, Nzakizwanayo J, Milo S, et al. Bacterial biofilm formation on indwelling urethral catheters. *Lett Appl Microbiol*. 2019;68(4):277–293. doi:10.1111/lam.13144
29. Ijaz M, Zafar M, Islam A, Afsheen S, Iqbal T. A review on antibacterial properties of biologically synthesized zinc oxide nanostructures. *J Inorg Organomet Polym Mater*. 2020;30:2815–2826. doi:10.1007/s10904-020-01603-9
30. Mazitova G, Kienskaya K, Ivanova D, Belova I, Butorova I, Sardushkin M. Synthesis and properties of zinc oxide nanoparticles: advances and prospects. *Rev J Chem*. 2019;9:127–152. doi:10.1134/S207997801902002X
31. Sweidan N, Abu Rayyan W, Mahmoud I, Ali L. Phytochemical analysis, antioxidant, and antimicrobial activities of Jordanian Pomegranate peels. *PLoS One*. 2023;18(11):e0295129. doi:10.1371/journal.pone.0295129
32. Klink MJ, Laloo N, Leudjo Taka A, Pakade VE, Monapathi ME, Modise JS. Synthesis, characterization and antimicrobial activity of zinc oxide nanoparticles against selected waterborne bacterial and yeast pathogens. *Molecules*. 2022;27(11):3532. doi:10.3390/molecules27113532
33. Yoshida T, Hatano T, Ito H, Okuda T. *Structural Diversity and Antimicrobial Activities of Ellagitannins. Chemistry and Biology of Ellagitannins: An Underestimated Class of Bioactive Plant Polyphenols*. World Scientific Publishing Co.; 2009:55–93.
34. Dimas KS, Pantazis P, Ramanujam R. Chios mastic gum: a plant-produced resin exhibiting numerous diverse pharmaceutical and biomedical properties. *vivo*. 2012;26(5):777–785.
35. Gortzi O, Rovoli M, Katsoulis K, et al. Study of stability, cytotoxic and antimicrobial activity of Chios mastic gum fractions (neutral, acidic) after encapsulation in liposomes. *Foods*. 2022;11(3):271. doi:10.3390/foods11030271
36. Goda RM, El-Baz AM, Khalaf EM, Alharbi NK, Elkhooly TA, Shohayeb MM. Combating bacterial biofilm formation in urinary catheter by green silver nanoparticle. *Antibiotics*. 2022;11(4):495. doi:10.3390/antibiotics11040495
37. Abdelghafar A, Yousef N, Askoura M. Zinc oxide nanoparticles reduce biofilm formation, synergize antibiotics action and attenuate *Staphylococcus aureus* virulence in host; an important message to clinicians. *BMC Microbiol*. 2022;22(1):244. doi:10.1186/s12866-022-02658-z
38. Babayevska N, Przysiecka L, Iatsunskyi I, et al. ZnO size and shape effect on antibacterial activity and cytotoxicity profile. *Sci Rep*. 2022;12(1):8148. doi:10.1038/s41598-022-12134-3
39. da Silva B L, Abuçafy MP, Berbel Manaia E, et al. Relationship between structure and antimicrobial activity of zinc oxide nanoparticles: an overview. *Int J Nanomed*;2019. 9395–9410. doi:10.2147/IJN.S216204
40. Y-j L, L-l H, Mustapha A, Li H, Hu Z, M-s L. Antibacterial activities of zinc oxide nanoparticles against *Escherichia coli* O157: H7. *J Appl Microbiol*. 2009;107(4):1193–1201. doi:10.1111/j.1365-2672.2009.04303.x
41. Diab R, Khameneh B, Joubert O, Duval R. Insights in nanoparticle-bacterium interactions: new frontiers to bypass bacterial resistance to antibiotics. *Curr Pharm Des*. 2015;21(28):4095–4105. doi:10.2174/138161282128150922175445
42. Choudhury R, Srivastava S. Zinc resistance mechanisms in bacteria. *Curr Sci*. 2001;2001:768–775.
43. Owolabi JB, Hekeu MM. Isolation and characterization of zinc resistant bacteria from a coil coating industrial wastewater treatment plant. *Int J Environ Sci*. 2015;5(5):1030–1042.

Infection and Drug Resistance

Publish your work in this journal

Infection and Drug Resistance is an international, peer-reviewed open-access journal that focuses on the optimal treatment of infection (bacterial, fungal and viral) and the development and institution of preventive strategies to minimize the development and spread of resistance. The journal is specifically concerned with the epidemiology of antibiotic resistance and the mechanisms of resistance development and diffusion in both hospitals and the community. The manuscript management system is completely online and includes a very quick and fair peer-review system, which is all easy to use. Visit <http://www.dovepress.com/testimonials.php> to read real quotes from published authors.

Submit your manuscript here: <https://www.dovepress.com/infection-and-drug-resistance-journal>

Dovepress
Taylor & Francis Group